Annual Meeting of Korean Society of Coastal and Ocean Engineers
Myong Ji University, 11 October 1997

Modelling Wave Propagation on a Turning Channel

J.L. Lee* and D.S. Baik**

INTRODUCTION

The interest in numerically-generated, Boundary-Fitted Coordinate Systems (BFCS) arises from the need for conforming the boundaries of the region in such way that boundary conditions can be accurately represented. The parabolic approximation method in solving wave phenomena is known to have a great merit as time-saving method. However, the method shows a disagreement for the wide angle and behind the structures since the numerical scheme used proceeds grid by grid along a main axis. When waves propagate through a turning channel, this disagreement also happens due to the turning angle of wave propagation and the zigzag boundaries on the Cartesian methods. The study of improvement for this disagreement is accomplished by using the boundary-fitted grid system to complicated region.

Boundary-fitted coordinates have been used extensively in propagating wave fields. Liu and Boissevain (1988) applied a non-conformal transformation to waves between two breakwaters. Kirby (1988) examined Liu and Boissevain's model by constructing the parabolic approximation in the transformed space. Recently, Dalrymple and Kirby (1994) developed the forward-propagation equations for Fourier-Galerkin and Chebyshev-tau models in conformal domains, and compared the results to exact solutions of waves in a circular channel. We develop wave models by mapping the wave equations of hyperbolic and parabolic types through the boundary-fitted coordinate transformation and compare the model results to exact solutions of waves either propagating or reflecting in a circular channel.

WAVE EQUATION

In the past two decades, prediction of nearshore waves took a new dimension with the introduction of the mild slope equation by Berkhoff (1972) which is capable of handling the combined effects of refraction and diffraction. Since then significant progress has been made in computational techniques as well as model capabilities, notably by Radder (1979), Copeland (1985), Ebersole et al. (1986), Yoo and O'Connor (1986), Madsen and Larsen (1987), Panchang (1988), and Dalrymple et al. (1989). However, no single model has been proven to be perfect or has clearly outperformed the others at present. The mild-slope equation of Berkhoff (1972) is expressed in terms of instaneous water surface velocity potential, ϕ as

---

* Assistant professor, Dept of Civil Engineering, Sung Kyun Kwan University, Suwon Campus, Suwon, Korea

** Graduate student, Dept of Civil Engineering, Sung Kyun Kwan University, Suwon Campus, Suwon, Korea

$$\nabla \cdot (CCg \nabla \phi) + k^2 CCg \phi = 0 \quad (1)$$

Writing $\Phi = \phi\sqrt{(CCg)}$ allows Eq. (1) to be cast into the form of a Helmholtz equation. Under the assumptions of slowly varying depth and small bottom slope, or high frequency wave propagation the equation for Φ may be approximated as, Radder (1979),

$$\nabla^2 \Phi + k_c^2 \Phi = 0 \quad (2)$$

where $k_c^2 = k^2 - \nabla^2 (CCg)^{0.5}/(CCg)^{0.5}$. Starting from Eq. (2), governing equations of parabolic and hyperbolic types will be derived.

BOUNDARY-FITTED COORDINATE SYSTEM

The basic idea of a boundary-fitted coordinate system is to have some coordinate line coincident with each boundary segment, analogous to the way in which lines of constant radial coordinate coincide with circles in a cylindrical coordinate system.

Parabolic Approach

In general curvilinear coordinates generated with $\nabla^2 \xi = 0$ and $\nabla^2 \eta = 0$, the non-conservative form of Laplacian operator can be written as

$$\nabla^2 \Phi = \frac{1}{J^2}\left[(x_\eta^2 + y_\eta^2)\Phi_{\xi\xi} - 2(x_\eta x_\xi + y_\xi y_\eta)\Phi_{\xi\eta} + (x_\xi^2 + y_\xi^2)\Phi_{\eta\eta}\right] \quad (3)$$

where J is the Jacobian of transformation given as

$$J = x_\xi y_\eta - x_\eta y_\xi \quad (4)$$

and subscripts indicate differentiation. Therefore, the Eq. (2) becomes

$$(x_\eta^2 + y_\eta^2)\Phi_{\xi\xi} - 2(x_\eta x_\xi + y_\xi y_\eta)\Phi_{\xi\eta} + (x_\xi^2 + y_\xi^2)\Phi_{\eta\eta} + J^2 k_c^2 \Phi = 0 \quad (5)$$

Equation (5) allows all computation to be done on a fixed square grid since it has been transformed so that the curvilinear coordinates replace the cartesian coordinates as the independent variables.

For the case of constant depth, substituting $\Phi = A(\xi, \eta)e^{ik_c\xi}$ into Eq. (5) yields

$$\alpha(A_{\xi\xi} + 2ik_c A_\xi - k_c^2 A) - 2\beta(ik_c A_\eta + A_{\xi\eta}) + \gamma A_{\eta\eta} + J^2 k_c^2 A = 0 \quad (6)$$

where $\alpha=(x_\eta^2+y_\eta^2)$, $\beta=(x_\eta x_\xi+y_\xi y_\eta)$ and $\gamma=(x_\xi^2+y_\xi^2)$.

If the waves propagate in the propagating direction ξ, the second derivative of A with respect to ξ can be neglected as

$$2i\alpha k_c A_\xi-2\beta(ik_c A_\eta+A_{\xi\eta})+\gamma A_{\eta\eta}+(J^2-\alpha)k_c^2 A=0 \tag{8}$$

which is the governing equation in the conformal domain. The derivatives are approximated in the finite difference form setting $\nabla\xi$ and $\nabla\eta=1$ as follows.

$$\begin{aligned}
A_\xi &= A_{i+1,j}-A_{i,j}\\
A_\eta &= \frac{1}{4}(A_{i,j+1}-A_{i,j-1}+A_{i+1,j+1}-A_{i+1,j-1})\\
A_{\eta\eta} &= \frac{1}{2}(A_{i+1,j-1}-2A_{i+1,j}+A_{i+1,j+1})\\
A_{\xi\eta} &= \frac{1}{2}(A_{i+1,j+1}-A_{i,j+1}-A_{i+1,j-1}+A_{i,j-1})
\end{aligned} \tag{9}$$

Substituting into Eq. (8) yields

$$a_j A_{i,j-1}+b_j A_{i,j}+c_j A_{i,j-1}=d_{i,j} \tag{10}$$

where,

$$a_j=\left[\frac{\beta ik_c}{2}+\beta+\frac{\gamma}{2}\right]$$

$$\begin{aligned}
b_j &= \left[2\alpha ik_c-\gamma+\frac{(J^2-\alpha)k_c^2}{2}\right]\\
c_j &= \left[-\frac{\beta ik_c}{2}-\beta+\frac{\gamma}{2}\right]\\
d_{i,j} &= \left[\left(-\frac{\beta ik_c}{2}-\frac{\gamma}{2}+\beta\right)A_{i,j-1}+\left\{2\alpha ik_c+\gamma-\frac{(J^2-\alpha)k_c^2}{2}\right\}A_{i,j}+\left(\frac{\beta ik_c}{2}-\frac{\gamma}{2}-\beta\right)A_{i,j+1}\right]
\end{aligned} \tag{11}$$

Equation (10) can be described in a trigonal matrix form as

$$\begin{bmatrix} b_1 & c_1 & & & \\ a_2 & b_2 & c_2 & & \\ & a_3 & b_3 & c_3 & \\ & & & \ddots & \\ & & & a_{ny} & b_{ny} \end{bmatrix}\begin{bmatrix} A_1\\ A_2\\ A_3\\ \vdots\\ A_{ny}\end{bmatrix}=\begin{bmatrix} d_1-a_1\\ d_2\\ d_3\\ \vdots\\ d_{ny}-c_{ny}\end{bmatrix} \tag{12}$$

Hyperbolic Approach

The governing equation of hyperbolic type is derived from the mild slope Eq. (1) as a pair of first order equations as follows.

$$\frac{Cg}{C}\frac{\partial \eta}{\partial t} + \nabla Q = 0$$
$$\frac{\partial Q}{\partial t} + C\,Cg \nabla \eta = 0 \tag{13}$$

which is similar to those used for the solutions of the shallow water equations. Equation (13) is transformed from the Catesian $\{x, y\}$ space into an alternate $\{u, v\}$ as

$$\frac{Cg}{C}\frac{\partial \eta}{\partial t} - \frac{1}{J}(Q_{xv}y_u - Q_{xu}y_v + Q_{yu}x_v - Q_{yv}x_u) = 0$$
$$\frac{\partial Q_x}{\partial t} - \frac{CCg}{J}(\eta_v y_u - \eta_u y_v) = 0 \tag{14}$$
$$\frac{\partial Q_y}{\partial t} - \frac{CCg}{J}(\eta_u x_v - \eta_v x_u) = 0$$

The derivatives are approximated in the finite difference form as

$$\frac{\partial \eta}{\partial t} = \frac{1}{J}\{y_u(Q_{x i,j+1} - Q_{x i,j}) - y_v(Q_{x i+1,j} - Q_{x i,j})$$
$$+ x_v(Q_{y i+1,j} - Q_{y i,j}) - x_u(Q_{y i,j+1} - Q_{y i,j})\}$$
$$\frac{\partial Q_x}{\partial t} = \frac{CCg}{J}\{y_u(\eta_{i,j+1} - \eta_{i,j}) - y_v(\eta_{i+1,j} - \eta_{i,j})\} \tag{15}$$
$$\frac{\partial Q_y}{\partial t} = \frac{CCg}{J}\{x_v(\eta_{i+1,j} - \eta_{i,j}) - x_u(\eta_{i,j+1} - \eta_{i,j})\}$$

This set of finite difference equations in the confomal domain is solved by the explicit scheme.

RESULTS

Both wave models developed here are compared for a circular channel of constant depth lying between two radii r_1=75 and r_2=200m and covering 180° arc. The exact solution of wave field in a circular channel was described in Dalrymple et al. (1994) as

$$\phi(r, \theta) = \sum_{n=0}^{N} a_n F_n(r) e^{i\gamma_n \theta} \tag{16}$$

where $F_n = [Y'_{\gamma_n}(kr_1)J_{\gamma_n}(kr) - J'_{\gamma_n}(kr_1)Y_{\gamma_n}(kr)]$ with γ_n determined by satisfying

$$Y'_{\gamma_n}(kr_1)J'_{\gamma_n}(kr_2) - J'_{\gamma_n}(kr_1)Y'_{\gamma_n}(kr_2) = 0, \qquad n=1,2,\dots.N$$

to enforce a no-flux boundary condition on $r=r_1$ and $r=r_2$. The a_n values are given in the following integral form :

$$a_n = \frac{\int_{r_1}^{r_2} \phi(r,0) r^{-1} F_n \, dr}{\int_{r_1}^{r_2} r^{-1} F_n^2 \, dr} \tag{17}$$

where the upwave boundary condition $\phi(r,0)$ is given as 1.

The parabolic and hyperbolic model results are shown in Figs. 1a and 1b and compared with the analytic solution shown in Fig. 1c. The numerical results show excellent similarity of the analytic solution. The reflection from the outer wall is observed prominently at about 40° and 120° . For this cases, the wavenumber k is 0.301 m^{-1}, the dimensionless channel width is kw = 37.625 where w is the channel width. For this numerical solution, the numbers of computational grids to the x and y-directions used are nx=200, ny=25, respectively. If waves are blocked by a cross wall at 90° , the waves reflected off the wall propagate backward. Therefore, the parabolic method requires the backward calculation differently from the wave model of hyperbolic type, then the resulting wave field is obtained by the superposition of the incident wave and the wave reflected off the cross wall. Figure 2 shows a comparison of the numerical results from parabolic and hyperbolic models with the analytic solutions. The analytic solution of resulting wave field can be given as

$$\phi(r,\theta) = \sum_{n=0}^{N} a_n F_n(r) e^{i\gamma_n\theta} + \sum_{n=0}^{N} a_n F_n(r) e^{i\gamma_n(\pi-\theta)}, \qquad 0 \le \theta \le \frac{\pi}{2} \tag{18}$$

CONCLUTIONS

The wave models of hyperbolic and parabolic types has been developed through a conformal transformation. Both were compared with the analytic solutions of waves propagating through a circular channel of constant depth lying between two radii r_1 =75 and r_2 =200m and covering 180° arc. Comparison indicates that both methods provide accurate results. The computation was also performed for a downwave reflecting condition. The parabolic model can also simulate the reflecting wave field by backward calculation starting with downwave conditions approaching to the wall. When a cross wall was put at 90° , the resulting wave fields obtained from both wave models were in good agreement with the exact solutions.

REFERENCES

Berkhoff, J.C.W., 1972. Computation of combined refraction-diffraction, Proc. 13th ICCE, ASCE, pp.471-490.

Copeland, G.J.M. 1985. A practical alternative to the mild slope wave equation, Coastal Eng., 9: 125-149.

Dalrymple, R.A. and Kirby, J.T., 1994. Waves in an annular entrance channel, Proc. 24th ICCE, ASCE, Orlando, 128-141.

Dalrymple, R.A., Suh, K.D., Kirby, J.T., and Chae, J.W., 1989. Models for very wide-angle water waves and wave diffraction. Part 2. Irregular bathymetry, J. Fluid Mech. 201: 299-322.

Ebersole, B.A., Cialone, M.A. and Prater, M.D. 1986. Regional coastal processes numerical modeling system, Report 1, RCPWWAVE-A linear wave propagation model for engineering use, Technical report CERC-86-4, US Army Engineer WES, Vicksburg, Mississippi.

Kirby, J.T., 1988. Parabolic wave computation in non-orthogonal coordinate systems, J. Waterway, Port, Coastal and Ocean Engrg., 114, 673-685.

Liu P.L.-F. and Boissevain, P.L., 1988. Wave propagation between two breakwaters, J. Waterway, Port, Coastal and Ocean Engrg., 114, 237-247.

Madsen, P.A., and Larsen, J. 1987. An efficient finite-difference approach to the mild-slope equation, Coastal Eng., 11: 329-351.

Panchang, V.G., Cushman-Roisin, B., and Pearce, B.R. 1988. Combined refraction-diffraction of short-waves in large coastal regions, Coastal Eng., 12:133-156.

Radder A.C. 1979. On the parabolic equation for water-wave propagation, J. Fluid Mech., 95: 159-176.

Yoo, D., and O'Connor, B.A. 1986. Mathematical modeling of wave-induced nearshore circulations, Proc. 20th ICCE, ASCE, pp.1667-1681.

(a)

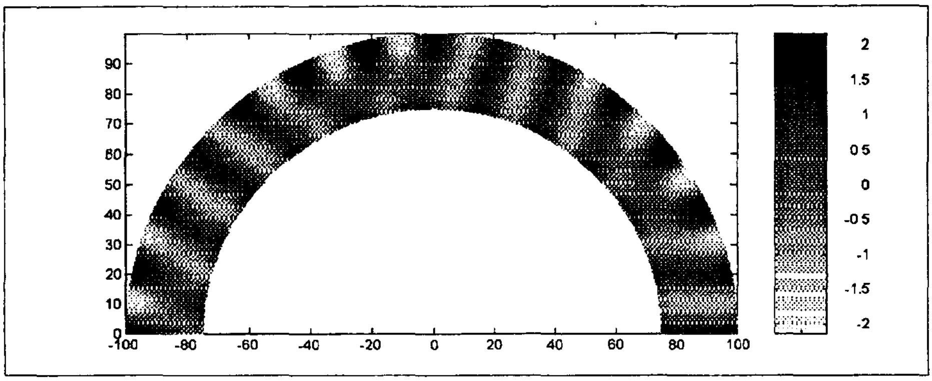

(b)

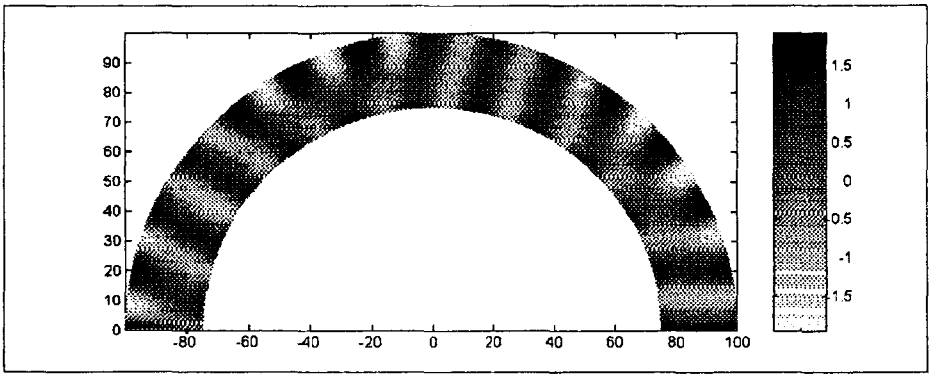

(c)

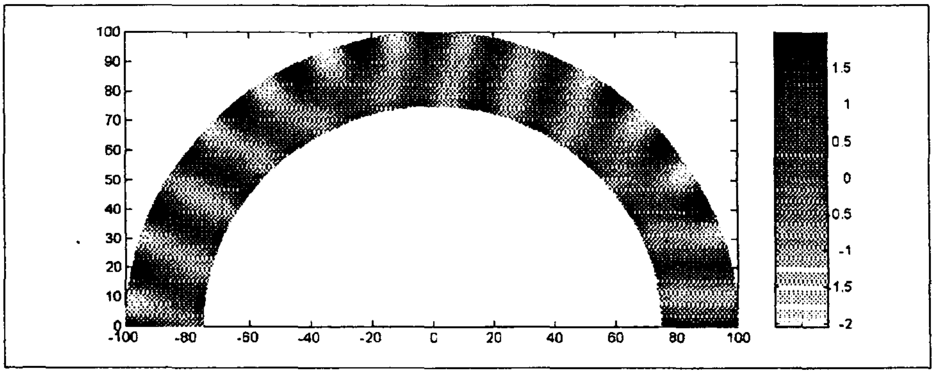

Fig. 1 Comparison of a) parabolic and b) hyperbolic model results to b) analytic solutions for the case of 180° arc.

(a)

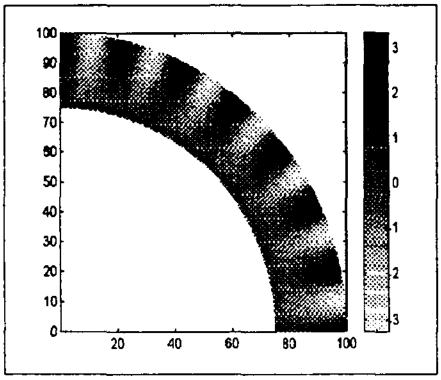

(b)

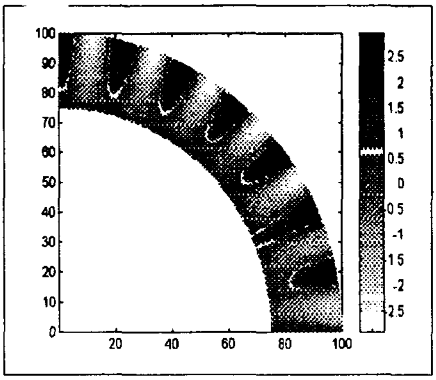

(c)

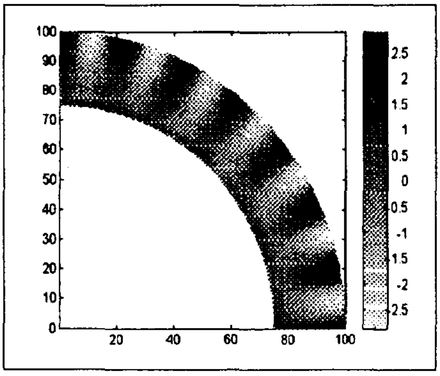

Fig. 2 Comparison of a) parabolic and b) hyperbolic model results to c) analytic solutions for the case of 90° cross wall.